

1

2

3

4

## $\Phi$ -Order kinetics of photoreversible–drug reactions

5

6

7

8

Mounir Maafi\* and Wassila Maafi

9

10 *Leicester School of Pharmacy, De Montfort University, The Gateway, Leicester, LE1 9BH, UK*

11

12

13 *Background:* Drug photodegradation data are usually treated by zero-, first- or second-  
14 order kinetic equations. Such treatments would lack reliability since the aforementioned  
15 equations have been originally developed for pure thermal reactions. In this respect, it has  
16 recently been shown that unimolecular photodegradations obey  $\Phi$ -order kinetics (Maafi  
17 and Maafi, 2013). However, no similar information is, thus far, available for other reactions  
18 including photoreversible AB(2 $\Phi$ ) systems. This paper aims at filling this gap for AB(2 $\Phi$ )  
19 kinetics.

20

21 *Methods:* Runge–Kutta numerical integration data for photoreversible reactions traces were  
22 combined with a template equation in order to derive an optimized (semi-empirical)  
23 integrated rate-law equation for AB(2 $\Phi$ ) reactions. The proposed model equation was test  
24 by examining its ability to fit synthetic Runge–Kutta data that have not been used for the  
25 optimization. The obtained fitting parameters are then compared to their theoretical  
26 counterparts.

27

28 *Results:* Both an integrated rate-law and an analytical equation for the overall reaction  
29 rate-constant were set for photoreversible drug reactions. The values of overall reaction  
30 rate-constant and initial velocity obtained theoretically correlated well with those obtained  
31 by fitting the kinetic traces of reactions with the derived integrated rate-law. AB(2 $\Phi$ )  
32 photodegradation reactions have been proven to obey  $\Phi$ -order kinetics. The equation  
33 proposed describes faithfully their kinetic behaviour in solution. The formula of the overall  
34 rate-constant involves both reagents characteristics and experimental parameters. These

35 equations facilitated the rationalisation and prediction of the individual effects of each  
36 reaction parameter. Specially, our results proved a self-photostabilisation with increasing  
37 initial drug-concentration and demonstrated the potential for actinometry of drugs obeying  
38 AB(2Φ) mechanism.

39

40

41

42 *Key words:* drugs photodegradation, kinetics modelling, AB photosystems, actinometry.

43

44 Corresponding author. Tel.: +44 116 257 7704; fax: +44 116 257 7287.

45 E-mail address: [mmaafi@dmu.ac.uk](mailto:mmaafi@dmu.ac.uk) (M.Maafi)

46

## 47 1. Introduction

48

49 The ICH recommendations for photostability testing of drugs and formulations (ICH, 1996) do  
50 not provide clear specifications or protocols on the treatment and analysis of the kinetic  
51 data of drug photodegradations. In the literature, the photokinetic data of the initial drug,  
52 usually extracted by a separation method, were treated according to the well-known  
53 classical zeroth-, first- or second-order kinetic model equations (Ming, 2012; Piechocki and  
54 Thoma, 2010; Tashtoush et al., 2008; Tonnesen, 2004; Albin and Fasani, 1998). These three kinetic  
55 options were used irrespective of the photochemical overall mechanism governing the drug  
56 and its photoproducts, and despite the fact that the aforementioned equations were  
57 originally developed for pure thermal reactions. It is also noticeable that most often the  
58 application of this approach meant that only data corresponding to the early stages of the  
59 reaction (up to the half-life time) were effectively used for the kinetic treatment (Piechocki  
60 and Thoma, 2010). In addition, the determined overall rate-constants of drug  
61 photodegradation reaction could neither be compared to those obtained by other studies or  
62 lead to the determination of the photochemical quantum yield of the reaction (the overall  
63 rate-constant and the quantum yield are generally achieved by separate experiments).

64

65 Recently (Maafi and Maafi, 2013; Maafi, 2010; Maafi and Brown, 2007), it has been shown  
66 that a drug unimolecular  $AB(1\Phi)$  photodegradation reaction, where the initial species (A)  
67 phototransforms into a product (B) with an efficiency  $\Phi_{A\rightarrow B}$ , obeys a specific kinetic order,  
68 the so-called  $\Phi$ -order, that significantly differs from the mathematical formulation of 0<sup>th</sup>-,  
69 1<sup>st</sup>- and 2<sup>nd</sup>-order equations. The  $\Phi$ -order kinetic was found to describe well the whole set

70 of AB(1 $\Phi$ ) photodegradation data and readily allows the determination of the reaction  
71 photochemical quantum yield from the reaction overall rate–constant. Nonetheless, the  
72 above findings have a limited application as they are specific to unimolecular drug  
73 photodegradations of the AB(1 $\Phi$ ) type.

74

75 Despite the relative mathematical similarity of the differential equations (DE) of drug  
76 photoreactions obeying more elaborate mechanisms than AB(1 $\Phi$ ), there are no known  
77 procedures to achieve their solutions, i.e. deriving the corresponding integrated rate–laws  
78 of such systems, through a closed–form integration (Maafi and Maafi, 2013; Maafi, 2010; Klan  
79 and Wirz, 2009; Mauser and Gauglitz, 1998). In this respect, it has been shown that it is not  
80 even possible to solve the DE of AB(1 $\Phi$ ) systems for the case where both (A and B) species  
81 absorb the incident light at a non–isosbestic wavelength (Maafi and Maafi, 2013).

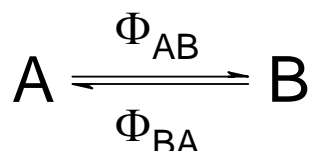
82

83 In order to circumvent this tedious problem, a new approach (Maafi and Maafi, 2013) was  
84 proposed to develop semi–empirical rate–law equations for drug photodegradation DEs  
85 that cannot conventionally be solved. It combines the results generated by a numerical  
86 method, such as Runge–Kutta (RK) method, to a plausible template equation. The various  
87 parameters involved in the rate–law equation would then be optimized and their analytical  
88 expressions defined.

89

90 In order to explore further the usefulness of the above approach, it is applied in the present  
91 study to propose an integrated rate-law equation for drugs that obey a photoreversible  
92 AB(2Φ) photodegradation reactions, as given in Scheme 1.

93



94

95 **Scheme 1.** Generic photodegradation drug-systems obeying an AB(2Φ) mechanism.

96

97 A wide range of important drugs and formulations undergo photoreversible reactions. A  
98 recent review (Ming, 2012) has listed a number of examples for drugs that degrade through  
99 E/Z photoisomerisation. Such drugs have varied therapeutic activities including but not  
100 limited to the treatment of depression (Tammilehto and Torniainen, 1989), Alzheimer disease  
101 (Azevedo Fihlo et al., 2010), neuroleptic disorders and psychosis (Stehfest et al., 2010; Maquille  
102 et al., 2010; Li Wan Po and Irwin, 1980), asthma (Al Omari et al., 2007; Radhakrishna et al., 2003)  
103 and infections (Lerner et al., 1988). In most cases, the produced photoisomer is much less or  
104 not biologically active compared to its counterpart, the initial drug isomer. Small  
105 photoisomerisable molecules have also been employed in neurobiology to target the GABA<sub>A</sub>  
106 receptor (Feliciano et al., 2010) for potential development of photo-nanomedicine and  
107 photodynamic materials. Another fast developing field is the incorporation of  
108 photoreversing systems in formulations and delivery systems such as photoresponsive  
109 hydrogels for biomedical applications (Tomatsu et al., 2011), photoresponsive materials for

110 drug delivery (Wohl and Engebensen, 2012) and light-triggered release from nanocarriers  
111 (Fomina et al., 2012).

112

113 Therefore, rationalising the kinetics of such photoreversible reactions is of importance to  
114 quantitatively evaluate the reactivity of the systems studied and shed light on their  
115 performance. This can best be achieved by the development of adequate integrated rate–  
116 laws.

## 117 2. Materials and methods

118

119 The method used here of deriving integrated rate-law equation for photodegradation drug  
120 systems whose differential equations cannot be integrated in a closed-form, has been  
121 recently developed in our team (Maafi and Maafi, 2013), and is applied here for AB(2 $\Phi$ )  
122 photodegradation reactions. It is based on the principle of using synthetically calculated  
123 data (representing the temporal variation of the species' concentrations or any other  
124 measurable variable such as absorbance), as model datasets to test, optimise and validate  
125 the proposed formula of the integrated rate-law and overall rate-constant. The RK-4  
126 calculation is fed with plausible reaction parameters to produce the kinetic traces. The  
127 reliability of RK-4 in solving differential equation makes it a powerful tool to deliver  
128 photodegradation reaction traces with high accuracy. The theoretical numerical integration  
129 used in this study has been constructed on the basis of the fourth-order Runge-Kutta (RK-  
130 4) method (results obtained from a homemade programme).

131

132 Around 50 traces were fitted with the proposed template formula for the integrated rate-  
133 law in order to optimise the analytical expressions of the exponential and the pre-  
134 logarithmic factors (*vide infra* Eqs. 2 and 3). This procedure is also meant to provide good  
135 indications on the limits of applicability of the proposed integrated rate-law equation. Once  
136 the complete formula has been derived, it has been tested against *c.a.* 100 more RK-4  
137 traces for validation and for application purposes.

138



139 The validation of the optimised integrated rate-law formula is achieved by not only  
140 recording a good fit of the RK-4 traces by the formula but also by ensuring that the values of  
141 reactions' overall rate-constants and initial velocities obtained from the fitting, differ by no  
142 more than 10 % of those values calculated using the theoretical equations.

143

144 A Levenberg-Marquardt iterative programme within the Origin 6.0 software package were  
145 used to run the non-linear fitting and the determination of the best fit curves.

146

147

148 **3. Results**

149

150 *3.1. The semi-empirical model for AB(2Φ) kinetics*

151

152 The differential equation expressing the time variation of the concentrations of species A  
153 and B ( $C_A(t)$  and  $C_B(t)$ , respectively, Scheme 1), considering that the solution, subjected to a  
154 monochromatic and continuous irradiation, is homogeneously and continuously stirred, the  
155 concentration of the excited-state is assumed to be negligible, the medium temperature is  
156 constant, and at the (non-isosbestic) irradiation wavelength ( $\lambda_{irr}$ ) species A and B absorb  
157 different amounts of light ( $P$ ), i.e., the absorption coefficients ( $\varepsilon$ ) of the species are different  
158 and have non-zero values ( $\varepsilon_A^{\lambda_{irr}} \neq \varepsilon_B^{\lambda_{irr}} \neq 0$ ), is (Maafi, 2008; Maafi and Brown, 2008)

159

$$\begin{aligned} \frac{dC_A(t)}{dt} &= -\frac{dC_B(t)}{dt} \\ &= \left( \Phi_{B \rightarrow A}^{\lambda_{irr}} \times \varepsilon_B^{\lambda_{irr}} \times C_B(t) - \Phi_{A \rightarrow B}^{\lambda_{irr}} \times \varepsilon_A^{\lambda_{irr}} \times C_A(t) \right) \times l_{\lambda_{irr}} \times P_{\lambda_{irr}} \times F_{\lambda_{irr}}(t) \quad (1) \end{aligned}$$

160

161 where  $\Phi^{\lambda_{irr}}$  are the forward and reverse quantum yields of the photochemical steps  
162 realised at the irradiation wavelength ( $\lambda_{irr}$ ),  $P_{\lambda_{irr}}$  is the radiant power,  $l_{\lambda_{irr}}$  is the optical  
163 path length of the irradiation beam inside the sample, and  $F_{\lambda_{irr}}$  the photokinetic factor.

164

165 Because  $F_{\lambda_{irr}}$  is a time dependent function, Eq.1 is not possibly integrated in a closed-form  
 166 (Maafi and Brown, 2008).

167

168 To circumvent this situation, the model equation previously developed for the unimolecular  
 169 photoreaction AB(1Φ), (Maafi, 2010; Maafi and Brown, 2007) which has been obtained by a  
 170 closed-form integration, can be used as a template to approach the model equation for  
 171 AB(2Φ) kinetics. Provided that irradiation ( $\lambda_{irr}$ ) and observation ( $\lambda_{obs}$ ) wavelengths are  
 172 clearly set (to define the specific  $\lambda_{irr}/\lambda_{obs}$  condition), an expression (Eq.2) can be proposed  
 173 as an integrated rate-law that describes the time evolution of the observed total  
 174 absorbance of the medium,  $A_{tot}^{\lambda_{irr}/\lambda_{obs}}(t)$ , for an AB(2Φ) system.

175

$$A_{tot}^{\lambda_{irr}/\lambda_{obs}}(t) = A_{tot}^{\lambda_{irr}/\lambda_{obs}}(pss) + \frac{A_{tot}^{\lambda_{irr}/\lambda_{obs}}(0) - A_{tot}^{\lambda_{irr}/\lambda_{obs}}(pss)}{A_{tot}^{\lambda_{irr}/\lambda_{irr}}(0) - A_{tot}^{\lambda_{irr}/\lambda_{irr}}(pss)} \times \frac{l_{\lambda_{obs}}}{l_{\lambda_{irr}}} \times \text{Log} \left[ 1 + \left( 10^{\left[ \left( \frac{A_{tot}^{\lambda_{irr}/\lambda_{irr}}(0) - A_{tot}^{\lambda_{irr}/\lambda_{irr}}(pss)}{A_{tot}^{\lambda_{irr}/\lambda_{irr}}(0) - A_{tot}^{\lambda_{irr}/\lambda_{irr}}(pss)} \right) \times \frac{l_{\lambda_{irr}}}{l_{\lambda_{obs}}} \right] - 1 \right) \times e^{-k_{A \rightarrow B}^{\lambda_{irr}} \times t} \right] \quad (2)$$

176

177 In this mathematical description, it is assumed that experimental measurements ( $A_{tot}$ ) of  
 178 spectroscopic and kinetic data are achieved under the observation ( $l_{\lambda_{obs}}$ ) and not the  
 179 excitation ( $l_{\lambda_{irr}}$ ) conditions (with  $l_{\lambda_{obs}}$  being the optical path length of the monitoring light  
 180 inside the sample). It is important to notice that these optical path lengths ( $l_{\lambda_{irr}}$  and  $l_{\lambda_{obs}}$ )

181 may not be equal, and the absorbance of the medium in the excitation conditions (i.e.  
182 measured along  $l_{\lambda_{irr}}$ ) may not be directly accessible.

183

184 The coefficients  $A_{tot}^{\lambda_{irr}/\lambda_{obs}}(t)$ ,  $A_{tot}^{\lambda_{irr}/\lambda_{obs}}(0)$ ,  $A_{tot}^{\lambda_{irr}/\lambda_{obs}}(pss)$ ,  $A_{tot}^{\lambda_{irr}/\lambda_{irr}}(0)$  and  $A_{tot}^{\lambda_{irr}/\lambda_{irr}}(pss)$   
185 in Eq.2 are the measured total absorbances of the medium (along  $l_{\lambda_{obs}}$ ) respectively  
186 recorded at reaction time  $t$ , at the initial time ( $t = 0$ ) and at the photostationary state,  $pss$   
187 (where  $t = \infty$ ), when the reaction medium is irradiated at a given irradiation wavelength and  
188 simultaneously monitored at either a different observation wavelength ( $\lambda_{irr}/\lambda_{obs}$ ) or at the  
189 same wavelength ( $\lambda_{irr}/\lambda_{irr}$ ). It is assumed that the reaction is quantitative and proceeds  
190 without by-products.

191

192 Eq.2 takes into account the presence of a  $pss$  by the introduction of the coefficient  
193  $A_{tot}(pss)$  in the formula previously set for AB(1 $\Phi$ ) systems (Maafi and Maafi, 2013).

194

195 The analytical expression of the exponential factor,  $k_{A\rightleftharpoons B}^{\lambda_{irr}}$  in Eq.2, which represents the  
196 overall reaction rate–constant, is given by

197

$$198 \quad k_{A\rightleftharpoons B}^{\lambda_{irr}} = \left( \Phi_{A\rightarrow B}^{\lambda_{irr}} \times \varepsilon_A^{\lambda_{irr}} + \Phi_{B\rightarrow A}^{\lambda_{irr}} \times \varepsilon_B^{\lambda_{irr}} \right) \times l_{\lambda_{irr}} \times P_{\lambda_{irr}} \times F_{\lambda_{irr}}(pss) \quad (3)$$

199

200 This expression of  $k_{A\rightleftharpoons B}^{\lambda_{irr}}$  has been worked out from the denominator of the equations of the  
 201 species concentrations at  $pss$  (where it is assumed that  $(dC/dt)_{pss} = 0$ ). This template flows  
 202 from an analogy with the case of an AB(2Φ) system considered under an isosbestic  
 203 irradiation (at  $\lambda_{isos}$ ) (Maafi and Brown, 2008; 2005a).

204

205 It is worth noting that the parameters involved in the formula of the overall rate-constant  
 206 correspond exclusively to the excitation conditions. This includes the photokinetic  
 207 factor,  $F_{\lambda_{irr}}(pss)$ , measured at  $pss$  (i.e. the observed total  $pss$  absorbance at  $\lambda_{irr}/\lambda_{irr}$  used  
 208 in Eq.4 has been multiplied by the ratio of the optical path lengths in order to convert it to  
 209 the total absorbance corresponding to the irradiation conditions, i.e. a measurement along  
 210 the optical path length  $\lambda_{irr}$ ).

211

$$F_{\lambda_{irr}}(pss) = \frac{1 - 10^{-\left(A_{tot}^{\lambda_{irr}/\lambda_{irr}}(pss) \times \frac{l_{\lambda_{irr}}}{l_{\lambda_{obs}}}\right)}}{A_{tot}^{\lambda_{irr}/\lambda_{irr}}(pss) \times \frac{l_{\lambda_{irr}}}{l_{\lambda_{obs}}}} \quad (4)$$

212

213

214

215

216

217 3.2. Optimization of the parameters and validation of the semi-empirical model

218

219 The validation of the semi-empirical model (Eq.2) is achieved by checking the model's  
220 performance against independently-generated RK-4 synthetic datasets for AB(2Φ) kinetics.

221

222 This step is mandatory since the efficiency of the new model can objectively be evaluated if  
223 the proposed integrated rate-law (Eq.2) is not only successful in fitting the RK-4 – simulated  
224 kinetic traces but also able to deliver the values of the model's parameter ( $k_{A\rightleftharpoons B}^{\lambda_{irr}}$ ) for a large  
225 number of simulated reactions involving a range of system and experimental specifications.

226

227 Selected sets of such specifications involved different values of (i) the absorption  
228 coefficients for the reactive species (i.e.,  $\varepsilon_A > \varepsilon_B$  and  $\varepsilon_A < \varepsilon_B$ ), (ii) the reaction quantum  
229 yields including cases where  $\Phi_{A\rightarrow B}^{\lambda_{irr}} = \Phi_{B\rightarrow A}^{\lambda_{irr}}$ , (iii) the optical path lengths for irradiation and  
230 observation, and (iv) radiant power (Table 1). Examples of calculated plots are shown in  
231 Figure 1.

232

233

234

235

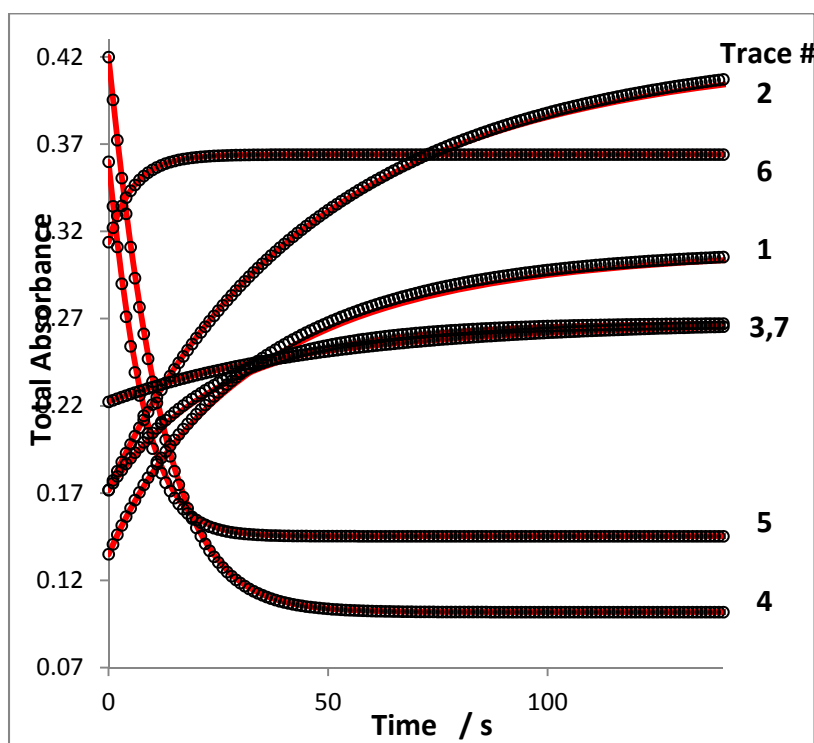
236

237 **Table 1** : Examples of reaction parameters used to feed RK-4 calculation of traces.

Attributes	$C_0^a$	$l_{\lambda_{irr}}^b$	$\varepsilon_A^{\lambda_{irr}}$	$\varepsilon_B^{\lambda_{irr}}$	$\Phi_{A \rightarrow B}^{\lambda_{irr}}$	$\Phi_{B \rightarrow A}^{\lambda_{irr}}$	$P_{\lambda_{irr}}$
Sample #	/ M	/ cm	/ $M^{-1} cm^{-1}$	/ $M^{-1} cm^{-1}$			/ $einstein s^{-1} dm^{-3}$
1	$2.0 \times 10^{-5}$	2	6748	32159	0.50	0.20	$1.0 \times 10^{-6}$
2	$2.0 \times 10^{-5}$	1	8587	30269	0.85	0.17	$9.3 \times 10^{-7}$
3	$2.0 \times 10^{-5}$	1	8587	30269	0.17	0.17	$3.4 \times 10^{-6}$
4	$7.5 \times 10^{-6}$	1	55984	10837	0.60	0.20	$1.5 \times 10^{-6}$
5	$1.0 \times 10^{-5}$	1.7	35984	10837	0.70	0.40	$2.0 \times 10^{-6}$
6	$6.0 \times 10^{-5}$	1	5231	30273	0.10	0.50	$7.0 \times 10^{-6}$
7	$1.0 \times 10^{-5}$	2	22231	71273	0.10	0.30	$3.0 \times 10^{-7}$

238 <sup>a</sup>:  $C_0 = C_A(0)$  and  $C_B(0) = 0$ . <sup>b</sup>:  $l_{\lambda_{irr}} = 1cm$ .

239

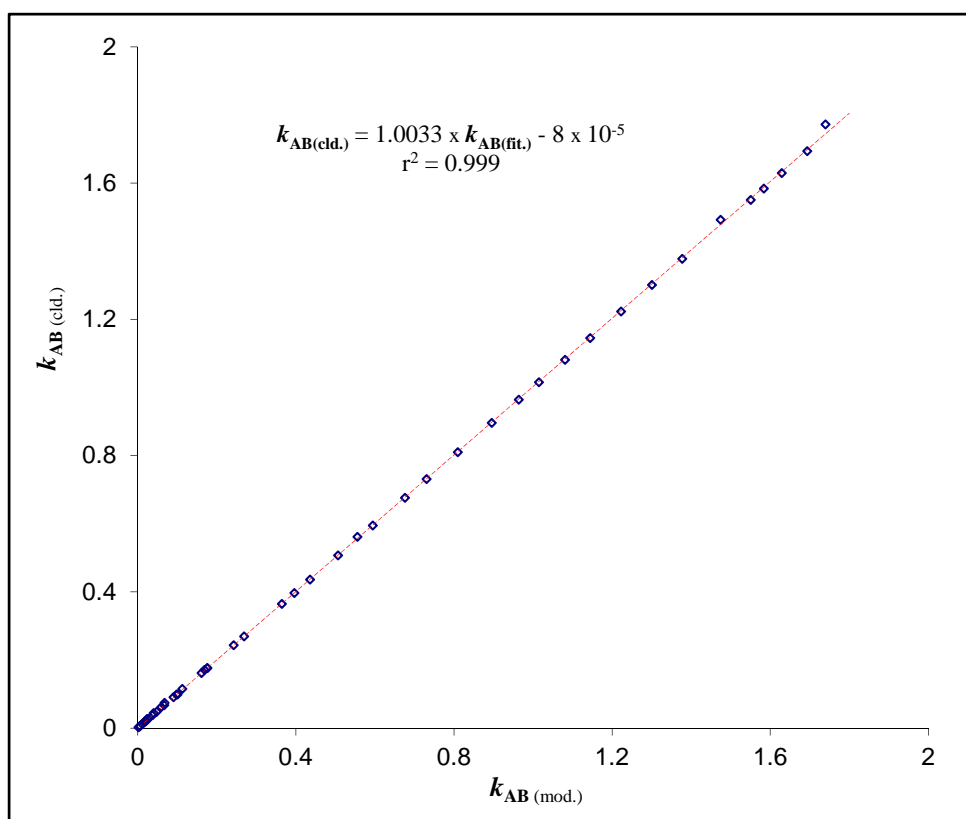


240

241 **Fig. 1.** Examples of the semi-empirical model, Eq.2 (lines), fitting of simulated RK-4 kinetic  
 242 traces (circles),  $A_{tot}^{\lambda_{irr}/\lambda_{irr}}$  vs. time, for AB(2 $\Phi$ ) photochemical reactions. The RK-4  
 243 calculations are based on the data of Table 1.

244 For the selected cases (> 150) of this study, the RK-4 data were all readily fitted by the  
 245 semi-empirical model. The overall reaction rate-constants ( $k_{A\rightleftharpoons B}^{\lambda_{irr}}$ ) values of this set spanned  
 246 over more than three orders of magnitude ranging between  $2 \times 10^{-3}$  and  $1.8 \text{ s}^{-1}$ . A good  
 247 agreement was found between  $k_{A\rightleftharpoons B}^{\lambda_{irr}}$  values obtained from the fitting ( $k_{A\rightleftharpoons B}^{\lambda_{irr}(mod.)}$ ) and  
 248 those calculated ( $k_{A\rightleftharpoons B}^{\lambda_{irr}(cld.)}$ ) using Eq.3 (Fig.2). It is also worth noting that a similar  
 249 conclusion has been reached for cases with high radiant power values (up to  $10^6$  times  
 250 higher than those used in Table 1).

251



252

253 **Fig. 2.** Correlation between the calculated values of overall rate-  
 254 constants of the reaction ( $k_{A\rightleftharpoons B}^{\lambda_{irr}(cld.)}$ ) against those obtained from the  
 255 fitting of RK-4 data with Eq.2 ( $k_{A\rightleftharpoons B}^{\lambda_{irr}(mod.)}$ ).  $k_{A\rightleftharpoons B}^{\lambda_{irr}}$  is expressed in  $\text{s}^{-1}$ .

256



257 Similarly, the initial velocities,  $v_0^{\lambda_{irr}/\lambda_{obs}}$ , of the photoreactions have also been calculated  
 258 and compared.

259

260 The theoretical initial velocity equation is derived from Eq.1 (written here for the reaction  
 261 medium absorbances) at  $t = 0$ ,  $(dA_{tot}/dt)_{t=0}$  (Maafi and Brown, 2008; 2005a), as

262

$$v_{0(cld.)}^{\lambda_{irr}/\lambda_{obs}} = (\varepsilon_B^{\lambda_{obs}} - \varepsilon_A^{\lambda_{obs}}) \times l_{\lambda_{obs}} \times \Phi_{A \rightarrow B}^{\lambda_{irr}} \times \varepsilon_A^{\lambda_{irr}} \times l_{\lambda_{irr}} \times P_{\lambda_{irr}} \times F_{\lambda_{irr}}(0) \times C_0 \quad (5a)$$

263

264 where  $F_{\lambda_{irr}}(0)$  is calculated using the initial absorbance,  $A_{tot}^{\lambda_{irr}/\lambda_{irr}}(0)$  (i.e. replacing  
 265  $A_{tot}^{\lambda_{irr}/\lambda_{irr}}(pss)$  in Eq.4). The values of the calculated initial velocity ( $v_{0(cld.)}^{\lambda_{irr}/\lambda_{obs}}$ ) are obtained  
 266 by using Eq.5a and the corresponding values of its parameters (as given in Table 1).

267

268 The initial velocity values can also be determined by differentiation of the model equation  
 269 (Eq.2) at the initial time,  $v_{0(mod.)}^{\lambda_{irr}/\lambda_{obs}}$ , as

270

$$v_{0(mod.)}^{\lambda_{irr}/\lambda_{obs}} = \left( \frac{dA_{tot}^{\lambda_{irr}/\lambda_{obs}}}{dt} \right)_0 = \frac{A_{tot}^{\lambda_{irr}/\lambda_{obs}}(0) - A_{tot}^{\lambda_{irr}/\lambda_{obs}}(pss)}{A_{tot}^{\lambda_{irr}/\lambda_{irr}}(0) - A_{tot}^{\lambda_{irr}/\lambda_{irr}}(pss)} \times \frac{k_{A \rightarrow B}^{\lambda_{irr}}}{l_{\lambda_{irr}} \times \ln(10)} \times \left( 10^{\left( A_{tot}^{\lambda_{irr}/\lambda_{irr}}(pss) - A_{tot}^{\lambda_{irr}/\lambda_{irr}}(0) \right) \times \frac{l_{\lambda_{irr}}}{l_{\lambda_{obs}} - 1}} - 1 \right) \quad (5b)$$

273 A good agreement is reached between pairs of  $v_0^{\lambda_{irr}/\lambda_{irr}}$  (or  $v_0^{\lambda_{irr}/\lambda_{obs}}$ ) values obtained  
274 from Eqs.5 (Fig.3). The straight line encompassing values ranging between  $2.2 \times 10^{-5}$  and  
275  $3.8 \times 10^{-1} \text{ s}^{-1}$  is characterized by a correlation coefficient close to unity and a small intercept  
276 value. Such range of  $v_0$  is thought to span a wide number of experimental values.

277

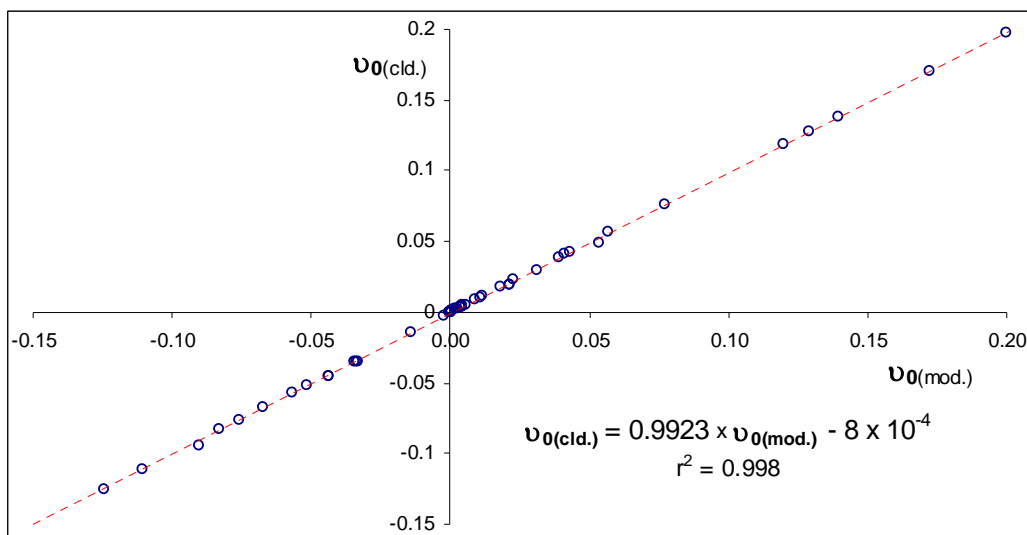
278 The errors between the two sets of values in Figs. 2 and 3 do not exceed 5 % whenever the  
279 value of  $F_{\lambda_{irr}}(pss)$  is higher than 1.2. This stands as a condition of reliability for the  
280 application of the semi-empirical model (Eq.2).

281

282 These findings strongly suggest that the semi-empirical model of the integrated rate-law is  
283 suitable to describe the kinetic behaviour of AB(2Φ) photochemical systems. Furthermore, it  
284 can provide reliable values for both overall reaction rate-constant and reaction initial  
285 velocity. This is achieved even before the reaction attributes (e.g.  $\epsilon$ ,  $\Phi$ ) have been  
286 determined.

287

288



289

290 **Fig. 3.** A plot of initial velocity values obtained theoretically (Eq.5a and Table 1)  
 291 against those generated by the fitting of the RK-4 trace with the semi-empirical  
 292 model (Eq.5b).  $v_0$  are expressed in  $\text{s}^{-1}$ .

293

294

295

#### 296 4. Discussion

297

298 The determination of integrated rate-law equations capable of faithfully describing  
 299 photolabile drug reactions including photoreversible systems is an area of research that  
 300 requires fundamental developments as there is number of drugs and/or technological  
 301 applications, that obey an AB(2Φ) mechanism, already exist or in development. The  
 302 common usage of the classical equations, set for 0<sup>th</sup>-, 1<sup>st</sup>- and 2<sup>nd</sup>- order thermal reaction  
 303 kinetics to treat photodegradation data of drugs, which has been thus far accepted as a  
 304 *standardized* good approximation, cannot be conceptually justified since both the frequency  
 305 and intensity of the light employed represent crucial parameters in the occurrence and

306 kinetic behaviour of the drug's reaction. This is mathematically conveyed by the presence of  
307 the time-dependent photokinetic factor that renders the differential equations and their  
308 solutions for photochemical reactions fundamentally different from those already  
309 established for the pure thermal processes (Maafi and Maafi, 2013; Maafi and Brown, 2007).

310

311 The application of thermal reaction kinetics to photodegradation reactions is not reliable as  
312 well from a practical viewpoint since most often only the data corresponding to the first  
313 section of the kinetic trace (reaching up to the half-life time) can effectively be utilized to  
314 define the reaction order (the rest of the data do not usually fit on the line). Caution has  
315 been raised about this approach as the data of a given reaction may well be fitted by the  
316 equations corresponding to two distinct thermal reaction-orders (Piechocki and Thoma,  
317 2010). In this context, the ICH Q1b recommendations (ICH, 1996) could benefit from a  
318 revision regarding issues on kinetic data treatment and the new replacement approach  
319 proposed in the present work.

320

321 The strategy adopted in a previous study (Maafi and Maafi, 2013), consisting of using RK-4  
322 simulated kinetic traces as background data for the generation of semi-empirical integrated  
323 rate-law equations for photochemical systems, as was readily applied to AB(1 $\Phi$ ) systems,  
324 has been successfully employed here for the photodegradation of drugs obeying AB(2 $\Phi$ )  
325 reactions. This approach, based on combining synthetic RK data of photoreactions and a  
326 convenient mathematical model for their integrated rate-law, may well represent a tool to  
327 explore further its potential usefulness and applicability for more extended drug

328 photodegradation processes whose differential equations cannot be integrated in a closed-  
329 form. Attempts in this field are being undertaken in our team.

330

331 The proposed semi-empirical model (Eq.2) fitted with high accuracy RK-4 synthetic data  
332 (Figs. 2) of AB(2Φ) kinetic systems subjected to continuous, non-isosbestic and  
333 monochromatic irradiations. The variety of the selected reaction attributes and  
334 experimental conditions (over 100 exemplars, in addition to those used for the development  
335 of Eq.2 and the analytical definition of its parameters) was aimed at spanning a large set of  
336 plausible situations, has proven the usefulness of Eq.2 in describing the kinetic behaviour of  
337 AB(2Φ) photodrugs with good accuracy. The threshold value imposed on  $F_{\lambda_{irr}}(\infty)$  ( $> 1.2$ )  
338 can easily be overcome experimentally by lowering the value of either the initial  
339 concentration of the drug or the optical path length of irradiation,  $l_{\lambda_{irr}}$  (Maafi and Maafi,  
340 2013).

341

342 Nevertheless, no limitations were found in terms of radiant power, absorption coefficients  
343 or quantum yield values. As a result, photoreversible drug degradation reactions are proven  
344 to obey Φ-order kinetics. Also, it is interesting to underline that the integrated rate-law for  
345 Φ-order AB(2Φ) reactions inherently depends on several parameters, namely  
346  $k_{AB}^{\lambda_{irr}}$ ,  $t$ ,  $\epsilon_{A \text{ or } B}^{\lambda_{irr}}$ ,  $\Phi_{A \rightarrow B \text{ or } B \rightarrow A}^{\lambda_{irr}}$  and  $C_{A \text{ or } B}(PSS)$ , conversely to the thermally reversible AB(2Δ)  
347 reaction rate-law that is exclusively expressed by  $k_{AB}$ ,  $t$  and  $C_{A \text{ or } B}(PSS)$  (Maafi and Brown,  
348 2005a).

349

350 Since the model Eq.2 has been developed using as a template the formula of AB(1Φ)  
 351 systems, and if one assumes that there is an analogy with thermal reaction kinetics (Maafi  
 352 and Brown, 2005a), then it should be possible to derive a single general equation to describe  
 353 the kinetic behaviour of any AB photoreaction performed at any observation/irradiation  
 354 conditions (Eq.6).

355

$$A_{tot}^{\lambda_{irr}/\lambda_{obs}}(t) = A_{tot}^{\lambda_{irr}/\lambda_{obs}}(\infty) + \frac{A_A^{\lambda_{irr}/\lambda_{obs}}(0) - A_{tot}^{\lambda_{irr}/\lambda_{obs}}(\infty)}{A_A^{\lambda_{irr}/\lambda_{irr}}(0) - A_{tot}^{\lambda_{irr}/\lambda_{irr}}(\infty)} \times \frac{l_{\lambda_{obs}}}{l_{\lambda_{irr}}} \\ \times \text{Log} \left[ 1 + \left( 10^{\left[ \left( A_A^{\lambda_{irr}/\lambda_{irr}}(0) - A_{tot}^{\lambda_{irr}/\lambda_{irr}}(\infty) \right) \times \frac{l_{\lambda_{irr}}}{l_{\lambda_{obs}}} \right]} - 1 \right) \times e^{-k_{A \rightleftharpoons B}^{\lambda_{irr}} \times t} \right] \quad (6a)$$

356

357 with

$$k_{A \rightleftharpoons B}^{\lambda_{irr}} = \left( \Phi_{A \rightarrow B}^{\lambda_{irr}} \times \varepsilon_A^{\lambda_{irr}} + \Phi_{B \rightarrow A}^{\lambda_{irr}} \times \varepsilon_B^{\lambda_{irr}} \right) \times l_{\lambda_{irr}} \times P_{\lambda_{irr}} \times F_{\lambda_{irr}}(\infty) \quad (6b)$$

359

360 Accordingly, for an AB(2Φ) system where both species (A and B) absorb at  $\lambda_{irr}$ , the  
 361 quantities  $A_{tot}^{\lambda_{irr}/\lambda_{obs}}(\infty)$  and  $F_{\lambda_{irr}}(\infty)$  in Eqs.6 will represent respectively  $A_{tot}^{\lambda_{irr}/\lambda_{obs}}(pss)$   
 362 and  $F_{\lambda_{irr}}(\infty)$ , which yields Eqs. 2 and 3. For a pure unimolecular AB(1Φ) reaction, where  
 363 only the initial compound absorbs the irradiation light,  $A_{tot}^{\lambda_{irr}/\lambda_{obs}}(\infty) = \Phi_{B \rightarrow A}^{\lambda_{irr}} = 0$  and  
 364  $F_{\lambda_{irr}}(\infty) = 2.3 \cong Ln(10)$ , Eqs.6 reduce to the model equations obtained through closed-  
 365 form integration for this system (Maafi, 2010; Maafi and Brown, 2007). For AB(1Φ) cases

366 where both A and B absorb at the irradiation wavelength (characterised by  $\varepsilon_{A \text{ or } B}^{\lambda_{irr}} \neq$   
367 0), then Eqs.6 derive the same equations previously obtained for this situation ( $\Phi_{B \rightarrow A}^{\lambda_{irr}} =$   
368 0 and  $F_{\lambda_{irr}}(\infty) = F_{\lambda_{irr}}(C_B(\infty))$ ) which is calculated using  $A_{tot}^{\lambda_{irr}/\lambda_{obs}}(\infty) = \varepsilon_B^{\lambda_{irr}} \times l_{\lambda_{irr}} \times$   
369  $C_A(0)$  (Maafi and Maafi, 2013). Finally, if A and B individual traces can be observed  
370 separately for any photoreversible system, then  $A_{tot}^{\lambda_{irr}/\lambda_{obs}}(\infty)$  would correspond to that of  
371 the particular observed species in all terms of Eqs.6 except for  $F_{\lambda_{irr}}(\infty)$ , which should be  
372 equal to that recorded for the medium at  $\lambda_{irr}$  (i. e.  $A_{tot}^{\lambda_{irr}/\lambda_{obs}}(\infty) = A_{tot}^{\lambda_{irr}/\lambda_{irr}}(\infty)$ , in Eq.6b).

373

374 Incidentally, the equations expressing the variations of either species concentration with  
375 reaction time can readily be also worked out from Eqs.6. It flows, from the above discussion,  
376 that Eqs.6 stand for the most general equations that are sufficient to fit the kinetic  
377 behaviour for AB photosystems as given in or part of Scheme 1.

378

379 It is also worthwhile noting that not only the overall reaction rate-constant but also the  
380 integrated rate-law (C(t)) equations of  $\Phi$ -order systems, explicitly depend on the  
381 absorption coefficients ( $\varepsilon$ ). This represents a major difference with the known expressions  
382 of classical reaction-orders.

383

384 In terms of elucidation of the kinetics based on spectral data there are two distinct  
385 situations. In the case where either the electronic spectrum of the photoproduct (or at least  
386  $\varepsilon_B^{\lambda_{irr}}$  is known) or the composition of the medium at the *pss* (i.e. the ratio,  $\rho =$

387  $C_A$  (PSS)/ $C_B$  (PSS), of the species *pss* concentrations. With  $\rho = 0$  for AB(1 $\Phi$ ) mechanisms)  
 388 is available, the determination of the absolute values of the forward and reverse quantum  
 389 yield values, are worked out using Eqs.7.

390

$$391 \quad \Phi_{A \rightarrow B}^{\lambda_{irr}} = \frac{v_0^{\lambda_{irr}/\lambda_{obs}}}{(\varepsilon_B^{\lambda_{obs}} - \varepsilon_A^{\lambda_{obs}}) \times \varepsilon_A^{\lambda_{irr}} \times F_0^{\lambda_{irr}} \times P_{\lambda_{irr}} \times l_{\lambda_{irr}} \times l_{\lambda_{obs}}} = \frac{k_{AB}^{\lambda_{irr}}}{\varepsilon_A^{\lambda_{irr}} \times F_{pss}^{\lambda_{irr}} \times P_{\lambda_{irr}} \times l_{\lambda_{irr}} \times (1+\rho)} \quad (7a)$$

392

$$393 \quad \Phi_{B \rightarrow A}^{\lambda_{irr}} = \frac{k_{AB}^{\lambda_{irr}}}{\varepsilon_B^{\lambda_{irr}} \times F_{pss}^{\lambda_{irr}} \times P_{\lambda_{irr}} \times l_{\lambda_{irr}}} - \frac{\varepsilon_A^{\lambda_{irr}} \times \Phi_{A \rightarrow B}^{\lambda_{irr}}}{\varepsilon_B^{\lambda_{irr}}} = \frac{\varepsilon_A^{\lambda_{irr}} \times \Phi_{AB}^{\lambda_{irr}} \times \rho}{\varepsilon_B^{\lambda_{irr}}} \quad (7b)$$

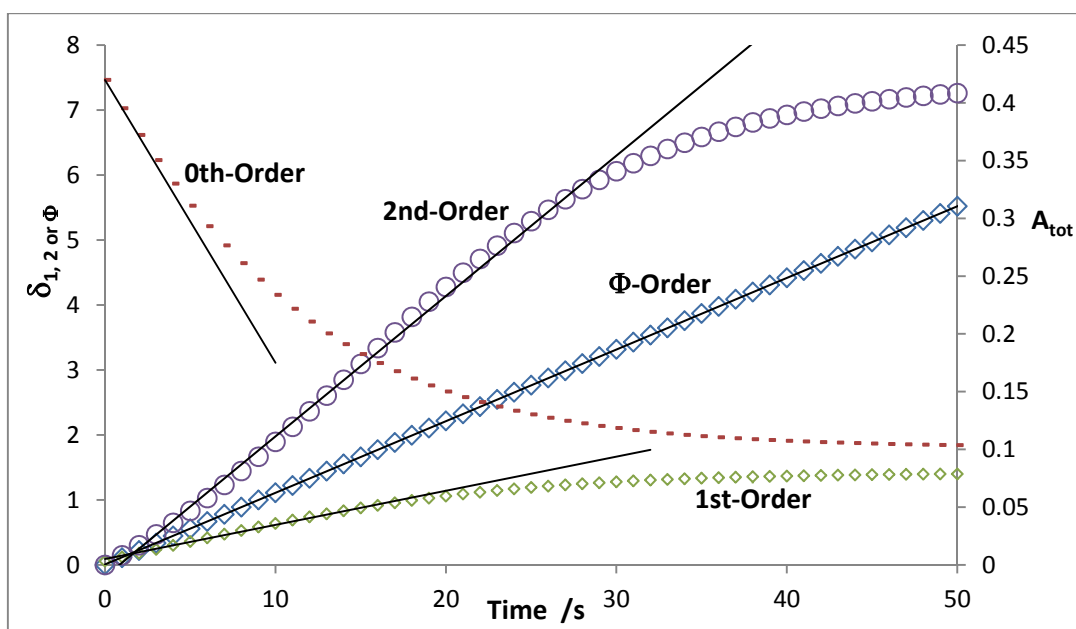
394

395 However, if only the spectroscopic data relative to reaction kinetics (e.g. UV-Vis traces)  
 396 obtained when the medium is subjected to non-isosbestic irradiation are available for drugs  
 397 where the electronic spectra of A and B totally overlap (this is the case for a majority of AB  
 398 drugs (Piechocki and Thoma, 2010; Piechocki and Thoma, 2010; Tashtoush et al., 2008;  
 399 Tonnesen, 2004), then the application of Eqs.6 would not be sufficient to determine the  
 400 values of the unknown parameters ( $\Phi_{A \rightarrow B}^{\lambda_{irr}}$ ,  $\Phi_{B \rightarrow A}^{\lambda_{irr}}$  and  $\varepsilon_B^{\lambda_{irr}}$ ) and/or ascertain whether the  
 401 reaction obeys an AB(1 $\Phi$ ) or an AB(2 $\Phi$ ) mechanism. This is a distinguishability problem  
 402 where the elucidation solution for the kinetics is degenerate (Maafi and Brown, 2005b). It is a  
 403 direct consequence of the generalization provided by Eqs.6. This consideration must be  
 404 taken into account in the treatment/interpretation of photodegradation reactions of drugs.  
 405 Therefore, the elucidation of the true mechanism, for this case, can only be achieved using  
 406 additional information that might be obtained by alternative means (until a pure  
 407 spectrokinetic method is developed).



408 Nonetheless, a good fitting of the experimental data with Eqs.2 or 6a certainly proves that  
 409 the reaction obeys AB  $\Phi$ -order kinetics. As shown in Fig.4, a linear relationship is only  
 410 obtained when the whole set of reaction data are treated according to  $\Phi$ -order kinetics. It is  
 411 also worth noticing that the data corresponding to the early stages of the reaction (*c.a.* the  
 412 half-life time) fit relatively well the models corresponding to 0<sup>th</sup>-, 1<sup>st</sup>- and 2<sup>nd</sup>-order  
 413 reactions.

414



415

416 **Fig. 4.** Treatment of the data corresponding to example 4 of Table 1 by models  
 417 corresponding to 0<sup>th</sup>-, 1<sup>st</sup>- , 2<sup>nd</sup>- and  $\Phi$ -order kinetics. The Y-axes are labelled either as  
 418  $\delta_{1,2 \text{ or } \Phi} = k_{A \rightleftharpoons B}^{\lambda_{irr}} \times t$  (left-hand side), correspond to the first terms of linear equations  
 419 describing 1<sup>st</sup>-, 2<sup>nd</sup>- or  $\Phi$ -order reactions, or  $A_{tot}$  (right-hand side), the total absorbance  
 420 assuming that the reaction obeys 0<sup>th</sup>-order kinetics. Solid lines correspond to the lines of best fit.  
 421

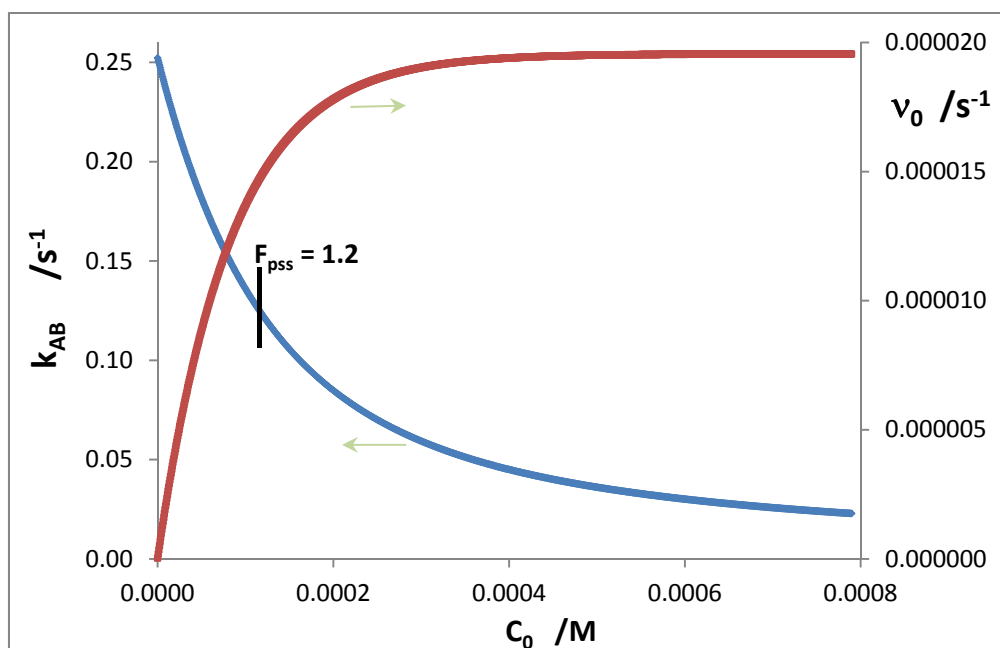
422

423 The expression of  $k_{A \rightleftharpoons B}^{\lambda_{irr}}$  (Eq.6b) indicates that the photodegradation overall rate-constant of  
 424 AB(2 $\Phi$ ) photodrugs depends inherently on the irradiation wavelength, the absorption  
 425 coefficients of mother compound and its photoproduct ( $\epsilon^{\lambda_{irr}}$ ), the forward and reverse

426 quantum yields ( $\Phi^{\lambda_{irr}}$ ), the optical path length travelled by the irradiation light inside the  
427 sample ( $l_{\lambda_{irr}}$ ), the radiant power ( $P_{\lambda_{irr}}$ ) and the photokinetic factor ( $F_{\lambda_{irr}}(\infty)$ ). This  
428 rationalises, for the first time, the set of factors affecting the overall rate–constant of such  
429 AB(2 $\Phi$ ) systems. It may contribute to a better interpretation of the literature data and  
430 reiterates the importance of using monochromatic irradiation for such photokinetic studies  
431 (Maafi and Maafi, 2013; Maafi, 2010). It is also worth noting that in the formula of  $k_{A\rightleftharpoons B}^{\lambda_{irr}}$ , the  
432 terms  $\varepsilon^{\lambda_{irr}} \times \Phi^{\lambda_{irr}}$  relative to A and B add up in a similar way to that observed for both  
433 photoreactions performed with isosbestic irradiation, and thermal reactions (Maafi, 2008;  
434 Maafi and Brown, 2008; 2005a). Furthermore, it indicates that the contribution of the latter  
435 term is balanced, in the formula of  $k_{A\rightleftharpoons B}^{\lambda_{irr}}$ , by that of  $F_{\lambda_{irr}}(\infty)$ .

436

437 The analytical formula also strongly implies that  $k_{A\rightleftharpoons B}^{\lambda_{irr}}$  directly depends on the initial  
438 concentration of the mother compound as implicitly stipulated in the expression of  
439  $F_{\lambda_{irr}}(\infty)$ . Therefore, it is evident that, assuming that all other experimental parameters and  
440 conditions are kept identical, an increase of the initial concentration would lead to a  
441 slowdown of the photoreaction and a self–stabilising effect is expected to occur on the  
442 photodegradation of the drug (Fig.5). This corroborates and explains a number of  
443 experimental observations reported in the literature (Piechocki and Thoma, 2010;  
444 Tonnesen, 2004). The initial velocity of the photoreaction is expected to increase with initial  
445 concentration of the drug as it depends on the non–linear factor  $\left(1 - 10^{-A_{tot}^{\lambda_{irr}}/\lambda_{irr}(0)}\right)$  as  
446 implicit in Eq.5a (Fig.5).



448

449 **Fig. 5.** Reduction of  $k_{A\rightleftharpoons B}^{\lambda_{irr}}$  and increase of  $v_0^{\lambda_{irr}/\lambda_{irr}}$  with increasing initial concentration of species  
 450 A. Data corresponding to example 6 of Table 1. The limit of applicability of Eqs.2 and 6 is  
 451 indicated by the vertical line ( $F_{\infty}^{\lambda_{irr}} = 1.2$ ); the curve of  $k_{A\rightleftharpoons B}^{\lambda_{irr}}$  after the horizontal line corresponds  
 452 to the assumption its formula applies.

453

454 Another effect of the variation of the drug's initial concentration is that of the half-life time

455 to equilibrium (or completion) of the reaction ( $t_{\frac{1}{2}\rightleftharpoons}$  corresponds to  $A_{tot}^{\lambda_{irr}/\lambda_{obs}} \left( t_{\frac{1}{2}\rightleftharpoons} \right) =$

456  $\pm \frac{A_{tot}^{\lambda_{irr}/\lambda_{obs}(0)} - A_{tot}^{\lambda_{irr}/\lambda_{obs}(\infty)}}{2}$ ). Indeed, for given reaction and set of  $\lambda_{irr}/\lambda_{obs}$  wavelengths,

457 Eq.8 suggests a non-linear evolution of  $t_{\frac{1}{2}\rightleftharpoons}(j)$  for  $j$  different initial concentrations,  $C_{A_j}(0)$ , as

458 well as for  $l_{\lambda_{irr}(j)}$  and  $l_{\lambda_{obs}(j)}$ .

459

460 Eq.8 makes  $t_{\frac{1}{2}\rightleftharpoons}$  of  $\Phi$ -order reactions very different from those concentration-independent

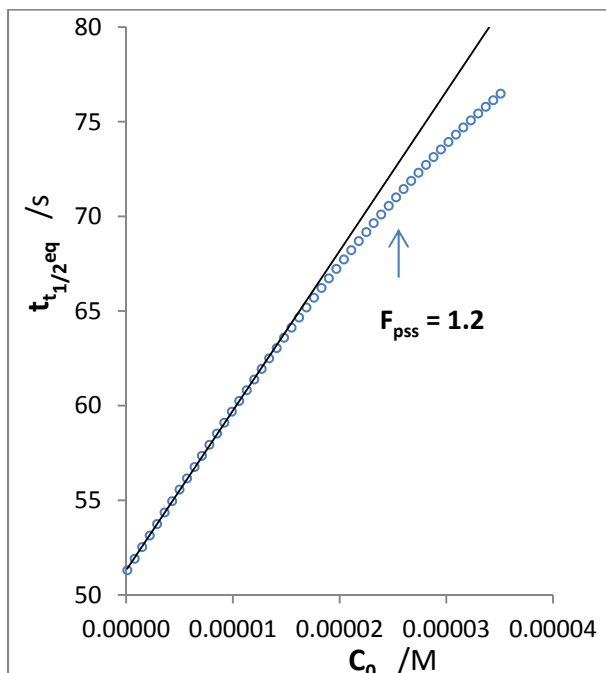
461 half-life times worked out for 0<sup>th</sup>- and 1<sup>st</sup>-order thermal reactions. It is also different from

462 that of 2<sup>nd</sup>-order reactions even though they share this property of being concentration-  
 463 dependent (but only  $t_{\frac{1}{2} \rightleftharpoons}$  of  $\Phi$ -order reactions depends on absorbance and optical path  
 464 length values). It is then essential to use reliable experimental values of end-of-reaction  
 465 ( $A_{tot}^{\lambda_{irr}/\lambda_{obs}}(\infty)$ ) absorbances for more accuracy.  $t_{\frac{1}{2} \rightleftharpoons}$  is found to vary quasi-linearly with  
 466 initial concentration for  $F_{pss}^{\lambda_{irr}} < 1.2$  for example 7 of Table 1 (Fig.5).

467

$$t_{\frac{1}{2} \rightleftharpoons} = \frac{-1}{k_{A \rightleftharpoons B}^{\lambda_{irr}}} \times \text{Ln} \left[ \frac{10^{\left[ \frac{\left( A_{tot}^{\lambda_{irr}/\lambda_{obs}}\left(t_{\frac{1}{2} \rightleftharpoons}\right) - A_{tot}^{\lambda_{irr}/\lambda_{obs}}(\infty) \right) \times \left( A_A^{\lambda_{irr}/\lambda_{irr}}(0) - A_{tot}^{\lambda_{irr}/\lambda_{irr}}(\infty) \right) \times l_{\lambda_{irr}}}{\left( A_A^{\lambda_{irr}/\lambda_{obs}}(0) - A_{tot}^{\lambda_{irr}/\lambda_{obs}}(\infty) \right) \times l_{\lambda_{obs}} \right] - 1}}{10^{\left[ \left( A_A^{\lambda_{irr}/\lambda_{irr}}(0) - A_{tot}^{\lambda_{irr}/\lambda_{irr}}(\infty) \right) \times \frac{l_{\lambda_{irr}}}{l_{\lambda_{obs}}} \right] - 1}} \right] \quad (8)$$

468



469

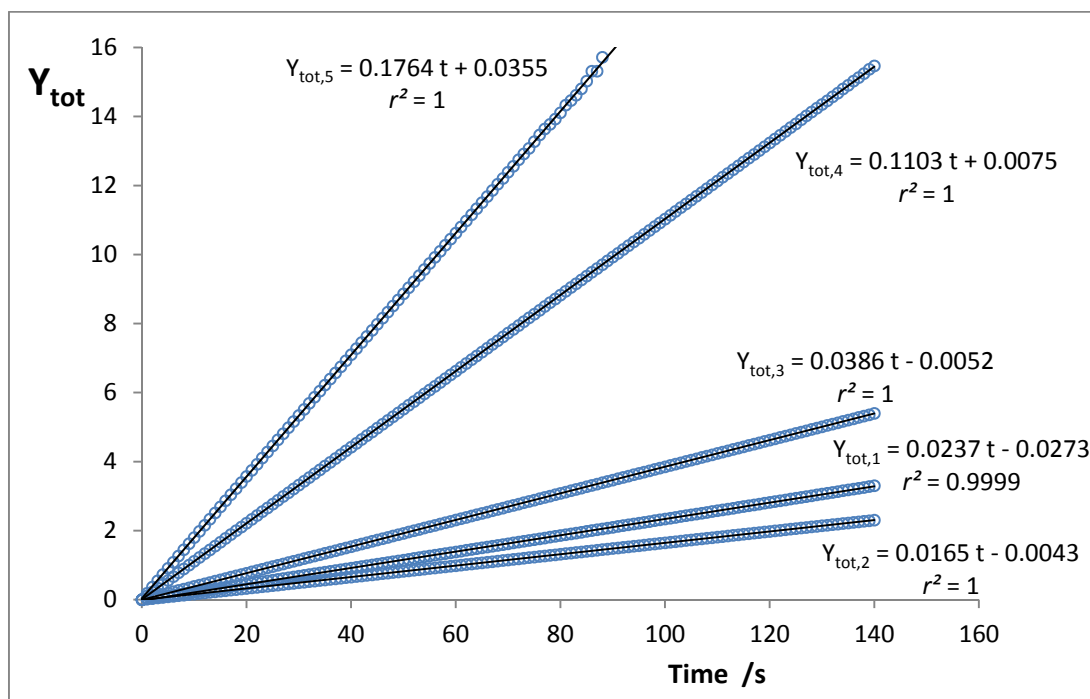
470 **Fig. 5.** Examples of the variation of the half-life time for an AB(2 $\Phi$ ) photodegradation  
 471 with initial drug concentration. The data points correspond to example 7 of Table 1.

472 In order to avoid non-linear fittings of the experimental traces, the overall rate-constant of  
 473 an AB(2Φ) reactions can be obtained as the slope of a line. The linear relationships (Eq.9),  
 474 obtained by rearranging Eq.6a to give the variation of  $A_{tot}^{\lambda_{irr}/\lambda_{obs}}(t)$  vs. time, might be found  
 475 much easier to handle and agrees with the classical pattern adopted for the treatment of  
 476 reaction kinetic data.

477

$$Y_{tot}^{\lambda_{irr}/\lambda_{obs}} = \text{Ln} \left[ \frac{10^{\left[ \left( A_A^{\lambda_{irr}/\lambda_{irr}(0)} - A_{tot}^{\lambda_{irr}/\lambda_{irr}(\infty)} \right) \times \frac{l_{\lambda_{irr}}}{l_{\lambda_{obs}}} \right] - 1}{\left[ \frac{\left( A_{tot}^{\lambda_{irr}/\lambda_{obs}(t)} - A_{tot}^{\lambda_{irr}/\lambda_{obs}(\infty)} \right) \times \left( A_A^{\lambda_{irr}/\lambda_{irr}(0)} - A_{tot}^{\lambda_{irr}/\lambda_{irr}(\infty)} \right) \times l_{\lambda_{irr}}}{\left( A_A^{\lambda_{irr}/\lambda_{obs}(0)} - A_{tot}^{\lambda_{irr}/\lambda_{obs}(\infty)} \right) \times l_{\lambda_{obs}} \right] - 1}} \right] = k_{A \rightleftharpoons B}^{\lambda_{irr}} \times t \quad (9)$$

478



479

480 **Fig. 6.** Φ-order plots ( $Y_{tot,n}^{\lambda_{irr}/\lambda_{obs}} = k_{A \rightleftharpoons B}^{\lambda_{irr}} \times t$ , Eq.9) for  $n = 1 - 5$  examples of Table 1.

481

482 Finally, the models presented in this study (Eqs.2 and 6a) would facilitate the development  
483 of new AB(2Φ) photodrug-based actinometers. For this purpose, the expected linear  
484 relationships between  $k_{A\rightleftharpoons B}^{\lambda_{irr}}$  or  $v_0^{\lambda_{irr}/\lambda_{obs}}$  with  $P_{\lambda_{irr}}$  (Eqs.5a and 6b), offer the possibility to  
485 monitor the variation of either parameter with radiant power. The collected linear data on  
486 the relationships for a given photodrug will be used for the development of an actinometric  
487 method spanning the wavelength range covering the whole absorption spectrum of the  
488 drug. This actinometric data can be used later to determine the radiant power of an  
489 unknown light source at given wavelengths. Such an approach can palliate the lack of drug-  
490 actinometers (Montali et al., 2006) and put forward alternatives to the quinine hydrochloride  
491 as proposed by ICH guidelines (ICH, 1996). The fact that the actinometric method presented  
492 in this study can be developed and implemented without requiring prior knowledge of any  
493 of the unknown reaction parameters (i.e.  $\epsilon_B^{\lambda_{irr}}$ ,  $\Phi_{A\rightarrow B}^{\lambda_{irr}}$  and  $\Phi_{B\rightarrow A}^{\lambda_{irr}}$ ), as long as the reaction  
494 obeys an AB mechanism, represents an undeniably important advantage.

495

496 Work is ongoing in our team to applying the new mathematical strategy to the  
497 photodegradation of AB(2Φ) drugs and exploring their actinometric potential (Maafi and  
498 Maafi, 2014).

499

500

501 **5. Conclusion**

502

503 The particular subject of drug photodegradation as well as photokinetics in general, an area  
504 of research with important industrial implications, requires some crucial developments with  
505 relation to valid and reliable integration rate–law equations able to describe and rationalize  
506 the kinetic behaviour of photodegradation reactions. This is crucially evident in the ICH  
507 recommendations set out in section Q1b, as the latter document lacks precise protocols  
508 and/or procedures aimed at the treatment of kinetic data, the determination of reactions’  
509 overall rate-constants, and/or quantum yields. Besides, the approaches based on zeroth,  
510 first or second order kinetics, though ubiquitous in the pharmaceutical literature, are  
511 arguably not appropriate to assess kinetic data corresponding to  $\Phi$ –order reactions.

512

513 The combination of a template equation and RK data, as has been proposed in the present  
514 investigation, has successfully led to establishing a useful equation that describes well the  
515 kinetics of drugs obeying AB(2 $\Phi$ ) mechanisms. It has also made possible a straightforward  
516 derivation of some fundamental parameters of the reaction including the photochemical  
517 quantum yields. This approach might contribute, as a new concept, to derive semi–empirical  
518 integrated rate–law equations suitable for drug photodegradations involving more extended  
519 mechanisms than that of the AB(2 $\Phi$ ) reaction.

520

521 Our results have also established that the magnitude of a photoreaction rate–constant is  
522 sensitive to all parameters related to AB reactions including the reactant and product

523 attributes ( $C_A(0)$ ,  $\varepsilon_A^{\lambda_{irr}}$ ,  $\varepsilon_B^{\lambda_{irr}}$ ,  $\Phi_{A \rightarrow B}^{\lambda_{irr}}$  and  $\Phi_{B \rightarrow A}^{\lambda_{irr}}$ ) as well as the experimental conditions  
524 ( $\lambda_{irr}$ ,  $P_{\lambda_{irr}}$ ,  $l_{\lambda_{irr}}$  and the irradiated volume of the solution). For the first time, a  
525 mathematical formulation allows to quantify the effect of each of the latter parameters.  
526 Furthermore, it offers an interesting tool for the development of new drug-actinometers for  
527 either or both the UV and Visible ranges.



528 **References**

529 **Albini, A., Fasani, E., 1998.** Drugs Photochemistry and Photostability. The Royal Society of  
530 Chemistry, Cambridge.

531 **Al Omari M.M., Zoubi R.M., Hasan E.I., Khader T.Z., Badwan A.A., 2007.** Effect of light and  
532 heat on the stability of montelukast in solution and in its solid state. J. Pharm. Biomed.  
533 Ana. 45(3), 465-471.

534 **Azevedo Fihlo, C.A., Giera, M., De Kanter, F.J.J., Niessen, W.M.A., Lingeman, H., Irth, H., 2010.**  
535 Photohuperzine A – A new photoisomer of huperzine A: structure elucidation, formation  
536 kinetics and activity assessment. J. Pharm. Biomed. Ana. 52, 190-194.

537 **Feliciano, M., Vylta, D., Medeiros, K.A., Chambers, J.J., 2010.** The GABA<sub>A</sub> receptor as a  
538 target for photochromic molecules. *Bioorg. Med. Chem.* 18, 7731-7738.

539 **Fomina N., Sankaranarayanan J., Almutairi A., 2012.** Photochemical mechanisms of light-  
540 triggered release from nanocarriers. *Advanced Drug Delivery Reviews.* 64, 1005-1020.

541 **ICH, 1996.** Guidance for industry Q1B photostability testing of new drug substances and  
542 products. Fed. Regist. 62, 27115-27112.

543 **Lerner, D.A., Bonnefond, G., Fabre, H., Mandrou, B., Buochberg., D.S.M., 1988.**  
544 Photodegradation paths of cefotaxime. *J. Pharm. Sci.* 77(8), 699-703.

545 **Klan, P., Wirz, J., 2009.** Photochemistry of organic compounds: from concept to practice.  
546 Postgraduate Chemistry Series, Wiley, Chichester.

547 **Li Wan Po, A., Irwin, W.J., 1980.** The photochemical stability of cis- and trans-isomers of  
548 tricyclic neuroleptic drugs. *J. Pharm. Pharmacol.* 32(1), 25-29.

549 **Maafi, M., 2008.** Useful spectrokinetic methods for the investigation of photochromic and  
550 thermo-photochromic spiropyran. *Molecules.* 13, 2260-2302.

551 **Maafi, M., 2010.** The potential of AB(1 $\Phi$ ) systems for direct actinometry. Diarylethenes as  
552 successful actinometers for the visible range. *Phys. Chem. Chem. Phys.* 12, 13248–  
553 13254.

554 **Maafi, M., and Brown, R.G., 2005a.** General analytical solutions for the kinetics of AB(k,  $\Phi$ )  
555 and ABC(k,  $\Phi$ ) systems. *Int. J. Chem. Kinet.* 37(3), 162-174.

556 **Maafi, M., and Brown, R.G., 2005b.** Analysis of diarylnaphthopyran kinetics. Degeneracy of  
557 the kinetic solution. *Int. J. Chem. Kinet.* 37, 717-727.

558 **Maafi, M., and Brown, R.G., 2007.** The kinetic model for AB(1 $\Phi$ ) systems. A Closed-form  
559 integration of the differential equation with a variable photokinetic factor. *J.*  
560 *Photochem. Photobiol. A: Chem.* 187, 319-324.

561 **Maafi, M., and Brown, R.G., 2008.** Kinetic analysis and kinetic elucidation options for  
562 AB(1k,2 $\Phi$ ) systems. *New Spectrokinetic methods for photochromes. Photochem.*  
563 *Photobiol. Sci.* 7, 1360 – 1372.

564 **Maafi, W., and Maafi, M., 2013.** Modelling Nifedipine Photodegradation, Photostability and  
565 Actinometric Properties. *Int. J. Pharm.* 456(1), 153-164.

566 **Maafi, W., and Maafi, M., 2014.** Montelukast photodegradation: Elucidation of  $\Phi$ -order  
567 kinetics, determination of quantum yields and application to actinometry. *Int. J. Pharm.*  
568 Under consideration.

569 **Maquille, A., Salembier, S., Herent, M.F., Jiwan, J.L.H., 2010.** Photodegradation of  
570 flupentixol in aqueous solution under irradiation at 254 nm: identification of the  
571 photoproducts generated. *J. Photochem. Photobiol. A:Chem.* 214, 224-229.

572 **Mauser, H., Gauglitz, G., 1998.** In *Comprehensive Chemical Kinetics, Vol. 36, Photokinetics:*  
573 *Theoretical Fundamentals and Applications*, Ed. R.G. Compton and G. Hancock. Elsevier:  
574 Amsterdam-New York-Oxford-Shannon-Singapore-Tokyo.

575 **Ming, L., 2012.** Organic Chemistry of drug degradation. RSC Drug Discovery Series No.29.  
576 The Royal Society of Chemistry, Cambridge.

577 **Montali, M., Credi, A., Prodi, L., Gandolfi, M.T., 2006.** Handbook of photochemistry (3rd  
578 Ed.). CRC Press – Taylor & Francis, Boca Raton-London-New York.

579 **Piechocki J.T., Thoma K., 2010.** Pharmaceutical Photostability and Photostabilisation  
580 Technology. Informa Healthcare, London.

581 **Radhakrishna T., Narasaraju A., Ramakrishna M., Satyanarayana A., 2003.** Simultaneous  
582 determination of montelukast and loratadine by HPLC and derivative  
583 spectrophotometric methods. J Pharm Biomed Anal. 31(2), 359-368.

584 **Stehfest, K., Ritter, E., Berndt, A., Bartl, F., Hegemann, P., 2010.** The Branched photocycle  
585 of the slow-cycling channelrhodopsin-2 mutant C128T. J. Mol. Biol. 398, 690-702.

586 **Tammilehto, S., Torniainen, K., 1989.** Photochemical stability of dothiepin in aqueous  
587 solution. Int. J. Pharm. 52(2),123-128.

588 **Tashtoush, B.M., Jakobson, E.L., Jakobsonx, M.K., 2008.** UVA is the major contributor to  
589 the photodegradation of tretinoin and isotretinoin: Implications for the development of  
590 improved pharmaceutical formulations. Int. J. Pharm. 352,123-128.

591 **Tomatsu I., Peng K., Kros A., 2011.** Photoresponsive hydrogels for biomedical applications.  
592 Advanced Drug Delivery Reviews. 63, 1257-1266.

593 **Tonnesen, H.H, 2004.** Photostability of Drugs and Drug Formulations (second Edition). CRC  
594 Press: London.

595 **Wohl B.M., Engebensen J.F.J., 2012.** Responsive layer-by-layer materials for drug delivery.  
596 Journal of Controlled Release. 158, 2-14.

597

598